Bacteria transfer by deformation through microfiltration membrane

Arthur Gaveau, Clémence Coetsier, Christine Roques, Patrice Bacchin, Etienne Dague, Christel Causserand

Bacteria transfer by deformation through microfiltration membrane

Arthur Gaveau[a], Clémence Coetsier[a], Christine Roques[a], Patrice Bacchin[a], Etienne Dague[b], Christel Causserand[a,*]

[a] *Laboratoire de Génie Chimique, Université de Toulouse, CNRS, INPT, UPS, Toulouse, France*
[b] *Centre National de la Recherche Scientifique (CNRS), Laboratoire d'Analyse et d'Architecture des Systèmes (LAAS), Toulouse, France*

A B S T R A C T

Living particles such as bacteria are able to transfer through membrane pores that are smaller than cell size due to the specific stiffness of this type of microorganism. This phenomenon can lead to a significant loss of selectivity in the filtration process, which is a major cause of concern in the sterilizing filtration step. This study investigates the retention of three bacteria strains: *Escherichia coli* CIP 54124, *Pseudomonas aeruginosa* CIP 103467 and *Staphylococcus aureus* CIP 53154 by model porous membranes for various operating conditions (transmembrane pressure, feed concentration and the physicochemical composition of filtered media with antibacterial agent added at sublethal concentration). The first part of this study is dedicated to defining the size and the nanomechanical properties of the envelope of the studied bacteria by microscopic techniques (Transmission electron microscopy & Atomic-force microscopy), in order to then explore the role of these quantifiable characteristics on the cell transfer through the pores by deformation mechanisms. Our results lead to the development of a numerical model to connect the observed retention efficiency of the filtration experiment and the microscopic information about individual particles.

1. Introduction

The production of drinking water or sterile fluid uses membrane processes to remove potentially pathogenic microorganisms, such as bacteria, present in suspension. With that aim, Ultrafiltration and Microfiltration are considered as efficient processes and it is accepted that membranes with pore sizes smaller than 0.22 μm can be used for clearance of biological particles contamination [1].

However, recent studies demonstrated that bacterial transfer through the membrane structure takes place during filtration operations, even if the pore size is significantly smaller than the bacteria cell size at rest in suspension [2–8]. Several reasons were put forward to explain these bacteria leaks through the membrane: firstly, the presence of defects in the membrane structure which appear during the membrane manufacture or ageing [9]; secondly, the biological nature of the filtered particles confers them the fitness to override the size-based selectivity mechanism. Living unicellular particles such as bacteria, yeasts, algae or red blood cells exhibit, in environmental conditions, a large variability of individual particle size, shape and envelope flexibility. Effectively, in the specific case of bacteria filtration, the cell size of the microorganisms is not the only parameter which determines the transfer through the membrane [10]. Recent works demonstrated that the shape of the bacteria cell [3] and the Gram type [7,8], which characterize the cell wall composition, are also important parameters that play a key role in the particle retention. The main part of bacteria species is classified as Gram-positive or Gram-negative according to their cell wall structure. The cell envelope of Gram-positive bacteria corresponds to a thick layer of peptidoglycan (cross-linked polymer) exposed outside of the cell membrane, whereas Gram-negative bacteria present a thin layer of peptidoglycan located between the cell membrane and the outer membrane (description available in a dedicated study [11]). This difference in structure, composition and organization of the cell wall and more specifically, the thickness of the peptidoglycan layer can lead to different retention rates during filtration tests: Gram-positive bacteria exhibiting a thicker peptidoglycan layer, are less deformable, and as a consequence, present higher retention rates [7,8].

Furthermore, it has to be noted that the physicochemical properties of the suspension used as feed in the filtration process, such as osmotic pressure [12], pH [13], concentration of nutrients [14] and exposure to antibacterial agents at sublethal concentrations [15], can result in changes in bacteria cell size, morphology or metabolic activity and can lead to a modification of the structure and the composition of the cell wall thus separation efficiency. Moreover, some antimicrobial molecules able to be present at low level in environment, are known for inducing alterations of the bacteria envelope and the mechanical

* Corresponding author.
E-mail address: caussera@chimie.ups-tlse.fr (C. Causserand).

http://dx.doi.org/10.1016/j.memsci.2016.10.023

properties such as elasticity of the cell wall, at concentrations without a loss of cell viability [16,17]. The impact of bacterial exposure to chemical agents on filtration retention efficiency has only been studied in a few cases of literature. For example, chemical treatment with molecules that impact the cell properties, such as fixation with glutaraldehyde [3] or cell wall alteration with antibiotics like beta-lactams [7], demonstrate a significant impact on the filtration selectivity. This can be due to, as supposed by the authors, the modification of the flexibility of the bacteria cell wall. Mycoplasma, bacteria without cell wall (with dimensions in the range of 0.2–1 μm) have been earlier demonstrated capable of penetrating 0.2 μm membrane filters, and even some 0.1 μm rated filters [18,19].

Direct observation of the deformation of the biological cell during the transfer through a membrane pore is only possible on a large scale and the study of blood cell constriction allows the production of numerical simulations of the dynamics of one individual particle transfer [20–24].

In the case of particles at a smaller scale, such as bacteria (with dimensions under 1–10 μm), there is still a need for better understanding of the key roles played by morphological properties of the individual particles on the selectivity mechanism. This is in order to describe the global behavior of a suspension during the filtration process.

The objective of this study is to evaluate the influence of several operating parameters on the transfer of bacteria that are in direct contact with the membrane interface, and to establish the correlation between bacteria cell morphology/mechanical properties and membrane retention efficiency. In addition, this work aimed to investigate the impact of antibiotics (at low concentration in the filtered medium) on the filtration selectivity, in order to explore the major concern of trace contaminants found in water resources and encountered in treatment processes.

The first part of this study focuses on the measurements of reliable quantitative information regarding the size, shape and the stiffness of challenged bacteria cells, with and without antibiotics, through microscopic observations. In that section, we used Atomic Force Microscopy (AFM) to analyze, at the nanoscale, living cell characteristics, such as morphological and nanomechanical properties of the cell envelope [25,26]. In the second part of this study, bacteria filtration was conducted with different operating conditions: various transmembrane pressures and bacterial cell concentrations in the feed (estimated in colony-forming units per mL: CFU/mL). To complete the analysis of bacteria transfer through membrane pore, a simple numerical approach will be proposed linking all the collected data (from bacterial cell morphology to behavior during filtration). This easy-to-use model aimed to anticipate the impact of the operative parameters on the filtration selectivity towards bacteria suspension and to provide a tool for membrane processes implementation that allows to select the optimal conditions to avoid downstream contamination.

The challenge operating conditions were chosen to allow the quantification of transfer magnitude of different bacteria strains, treated or not by non-lethal concentration of antibiotic, through membrane pores smaller than the expected dimensions of the bacteria. The selected membrane should have specific intrinsic characteristics such as calibrated pore size and geometry. For this reason, we have selected isopore track-etched membranes [27]. Performed for low filtered volumes, short filtration runs will provide direct measurements of bacteria transfer in conditions without relevant fouling in order to avoid enhancement of the retention by the deposit on the membrane surface.

2. Materials and methods

2.1. Microorganisms, culture and enumeration conditions

Three different bacterial strains were used for this experimental study: *Escherichia coli* (CIP 54124), *Pseudomonas aeruginosa* (CIP 103467) and *Staphylococcus aureus* (CIP 53154) from the Pasteur Institute Collection (Paris, France). These bacteria have been selected in order to cover species with different morphological and structural characteristics and for their implication in waterborne diseases and/or nosocomial infections.

For the preparation of the suspension used for this work, bacteria were grown aerobically on tryptone soy agar (Biomérieux, Crapone, France) plates at 37 °C for 24 h. This pre-culture was transferred on tryptone soy agar plate for another 24 h culture. Colonies from the second culture were suspended in sterile NaCl aqueous solution at 9 g/L (noted here as physiological solution) in order to obtain a concentration of around 10^8 CFU/mL controlled by optical density at 640 nm. Then, tenfold dilution series were realized to adjust the feed concentration to 10^4, 10^6 and 10^7 CFU/mL.

In order to evaluate the bacteria concentration in samples (feed and permeate samples collected during filtration experiments), tenfold dilution series were performed after homogenization and 1 mL of each dilution was deposited in a sterile Petri dish before adding 12–15 mL of melted tryptone soy agar medium previously cooled to 45 ± 1 °C.

Colony Forming Units (CFU) were enumerated after overnight incubation of the plates at 37 °C, considering only dilutions with counts between 30 and 300 CFU. For each sample collected in this study, bacteria enumeration was performed in duplicate.

2.2. Antibiotic treatment

Part of this project was to explore the impact of chemical agents, such as pharmaceuticals that can be found in the environment, on filtration selectivity towards bacteria. Specific molecules which induce morphological alteration, like antibiotics, have been selected with that aim. The bacteria suspensions were then treated with beta-lactam antibiotics: amoxicillin (Sigma Aldrich-A8523) for *E. coli* and *S. aureus*, or ticarcillin (Sigma Aldrich-T5639) for *P. aeruginosa*. This class of antibiotics avoids cross-linkages between the peptidoglycan polymer chains (the network responsible for the mechanical properties of the bacteria cell wall) and was used in this study at sub-inhibitory and sub-lethal concentrations to affect the stiffness of the bacterial cell wall without altering the viability and cultivability of the microorganisms.

In first instance, we aimed to determine the antibiotic concentration that will be added in the bacteria suspension without impairment of cell viability. Minimal Inhibitory and Bactericidal Concentrations (MIC and MBC) of the selected molecules were determined against the tested strains using a Mueller-Hinton broth (Biomérieux) in microtiter plates with agar dilution method [28], followed by a subculture on Mueller-Hinton agar (Biomérieux), as previously described [7]. The viability and the cultivability of the bacteria in suspension were then checked by numeration on trypcase soy agar after 180 min of contact with the selected antibiotic at MIC/2 concentration (amoxicillin: 1 μg/mL for *E. coli* and 0.05 μg/mL for *S. aureus*, or ticarcillin: 15 μg/mL for *P. aeruginosa*). In these conditions, no decrease of CFU counts was observed. Finally, for bacteria characterization steps or filtration run, the bacterial feed suspension at challenged concentrations was kept in contact or not (control) with the selected antibiotic at MIC/2 for 90 min in a physiological solution before the experiment.

2.3. Membrane

Polycarbonate microfiltration membranes used for this study are provided by Nuclepore – Whatman. According to manufacturer specification, they exhibit a narrow controlled pore size distribution with a nominal pore diameter of 0.4 μm, with porosity in the range of 4–20% and a membrane thickness of 20 μm. These membranes have been used as model material because of their well-defined pore geometry (cylindrical). In our study, the effective area of the micro-

filtration membrane was $1.34 \cdot 10^{-3}$ m^2.

A new membrane was used for each experimental run. Before the filtration experiment, the membrane was first disinfected by soaking in a solution of sodium hypochlorite at 200 ppm for 20 min. Then, sterile distilled water was filtered to rinse the membrane.

Prior to use, the integrity of the coupons used for bacterial filtration experiments has to be verified. The sampled membrane must validate a bubble point test and its hydraulic permeability must be consistent with the mean value measured for a large number of coupons (13,800 ± 1380 L/h m^2 bar). Bubble point was visually determined by firstly wetting the membrane with water and secondly replacing water by pressurized air in the retentate compartment. The air pressure was increased and the value at which the first bubble appeared in the permeate compartment was recorded. Membrane permeability was deduced from measurements of water flux at different transmembrane pressures. The slope of the curve water flux-pressure then obtained allowed the calculation of the permeability through the use of the Darcy Law. In this study, we experimentally determined the mean hydraulic permeability from measurements on more than 50 sampled membranes coupons. This mean value was 13,800 L/h m^2 bar and the acceptable range was arbitrary chosen at 10%. These two steps were achieved prior to each filtration experiment for each sampled membrane, in order to reject samples exhibiting abnormally large pores.

2.4. Experimental setup, filtration procedure and challenged conditions

The filtration experiments were performed in a dead-end mode, using a setup consisting of: a pressurized feed tank, a stirred dead-end filtration cell (Model 8050, Amicon – Millipore) and a sterilized chamber, used to collect the permeate. Each experiment was performed at room temperature under a laminar air flow, to prevent contamination. This setup enables easy disinfection and prior to filtration experiments, each piece of equipment was sterilized (20 min at 120 °C). Gentle stirring of the filtration cell (at 200 rpm) was used in order to homogenize the bacteria suspension in feed/retentate phase, no impact of this stirring on the filtration behavior (bacteria transfer and permeation flux) was pointed out.

In this study, the filtered volume of bacterial suspension should be relatively low in order to avoid a deposit formation on the membrane surface, which could interfere with the bacteria transfer through the membrane pore. The total filtered volume was set at 50 mL and collected in a sterile tube. TMP was selected in the range of 0.5–1.5 bar. This range was chosen to match the pressure used in water production plants, using membrane processes. The feed concentration (Cf) was selected in the range of 10^4 to 10^7 CFU/mL, in order to cover a large magnitude of loading rates with regard to guideline values ($1 \cdot 10^7$ particles per cm^2 membrane area) for the evaluation of sterilizing filters according to ASTM F838-05 [29]. The filtration medium was selected as a sterile physiological solution (denoted also as the control condition in this study), composed of ultra-pure water and 9 g/L of sodium chloride, in order to keep isotonic conditions for bacteria. Finally, the impact of the presence of antibiotics in the physiological solution was evaluated as the second chemical challenged condition.

Each experiment was performed three times for each challenge condition.

2.5. Transmission electron microscopy (TEM)

Suspension samples were prepared for TEM observation using the conventional negative staining procedure. Drops of bacteria suspension (20 µL), at a concentration of 10^7 CFU/mL were absorbed on Formvar carbon-coated grids for 2 min. The drops were then blotted and negatively stained with 1% (w/v) aqueous uranyl acetate for 1 min. The grids were then examined with a transmission electron microscope (Jeol JEM-1400) at 80 kV. Images were acquired using a digital camera (GatanOrius) at 8000× magnification. Then, cell size measurements were carried out for each strain and for the different chemical conditions (control conditions or after antibiotic treatment) for a total of 30 cells per condition using ImageJ image analysis software.

2.6. Atomic Force Microscopy (AFM)

2.6.1. Sample preparation for AFM experiments

Treated or untreated bacteria with antibiotics were concentrated by centrifugation, washed 2 times in physiological solution, and re-suspended in the physiological solution for immobilization on PolyEthylenImine (PEI) coated glass slides (prepared as previously described in the literature [30]). Freshly oxygen activated glass slides were covered by a 0.2% PEI solution in deionized water and left for incubation overnight. Then the glass slides were rinsed with 20 mL of ultrapure water and dried with nitrogen gas. A volume of 1 mL of the bacterial suspension was then dropped on the PEI-coated glass slide. This electrostatic immobilization method was used for rod-shaped bacteria, such as *E. coli* and *P. aeruginosa*. For the third bacterial strain, *S. aureus*, a specific immobilization method was required, due to the spherical shape of this microorganism. Then, physical entrapment was used to firmly immobilize the cells and withstand the lateral forces exerted by the scanning AFM tip. *S. aureus* cells were immobilized on polydimethylsiloxane (PDMS) stamps, prepared as described in the literature [31,32]. Briefly, freshly oxygen-activated microstructured PDMS stamps were covered with 100 µL of the *S. aureus* suspension and left for 15 min at room temperature. The cells were then trapped into the microstructures of the stamp by manual convective/capillary assembly and the size of the cavity used was the smallest available on the stamp with the wells of 1.5×1.5 μm^2. No drying procedure was required nor for the immobilization on the PEI slides nor on the PDMS stamps. Bacteria were always kept in solution (physiological solution) during the sample preparation and the AFM experiments.

2.6.2. AFM measures

For observations of the bacteria morphology on a nanoscale, acquisitions were performed on living cells in liquid medium at room temperature with a Nanowizard II (JPK instruments), using MLCT AUHW cantilever with nominal spring constant 0.01 N/m and pyramidal tips (Bruker). Before each experiment, the calibration was realized in a liquid medium (physiological solution) by measuring the sensitivity and the spring constant of the AFM tip. Vertical deflection images were recorded in the physiological solution buffer in contact mode to first localize the bacteria cell on the sample surface and then to observe the cell morphology. For stiffness measurements of the bacteria cell wall, the force-spectroscopy mode was used. Force maps of 32-by-32 force curves were recorded on a small area (0.04 μm^2) on top of the cells. Force curves were obtained for an applied force of 0.5 nN on the top of the bacteria cell surface. The force-distance curves recorded were transformed into force-indentation curves by subtracting the cantilever deflection on a solid surface. Then, the indentation curves were fitted with the Hertz model [33], which allows expressing the force as a function of the apparent Young Modulus of the surface (with a tip opening angle of 18° and the Poisson ratio arbitrary fixed to 0.5). For each condition, elasticity mapping of the bacteria cell wall was performed for a total of 9 cells. Each of the nine cells were collected from three individual suspensions, and from three independent cultures, in order to determine an average value.

3. Results and discussion

3.1. Bacterial cell observation

The first part of this study was dedicated to precisely defining the size and the nanomechanical properties of the selected bacteria cells.

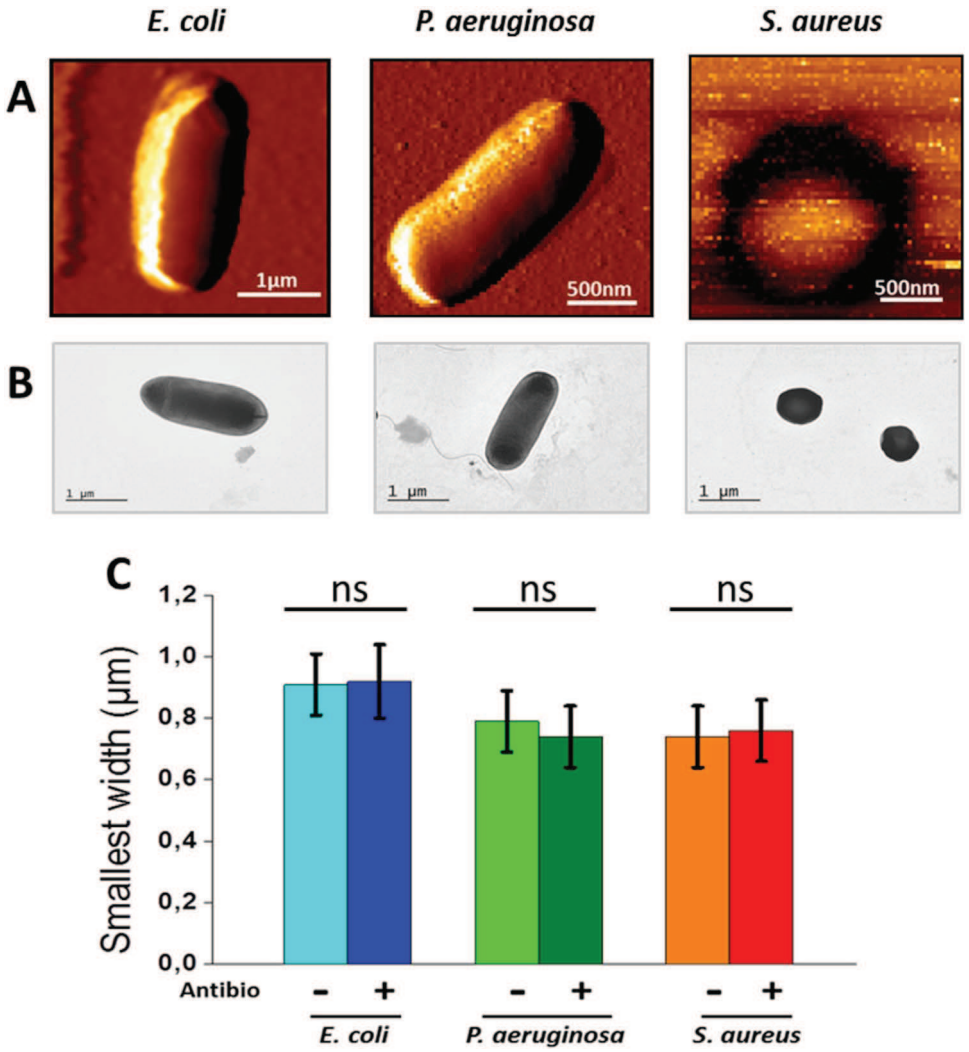

Fig. 1. Bacteria Morphology observed by AFM (A) and TEM (B and C). From left to right, morphology data of *E. coli* CIP 54124, *P. aeruginosa* CIP 103467 and *S. aureus* CIP 53154 respectively. A) AFM vertical deflection images (contact mode) of living bacteria cells measured in physiological solution. B) TEM images of individual bacteria cells observed at the same magnification (8000×) in physiological solution. C) Smallest width measured by TEM on untreated bacteria (−) and after antibiotic treatment (+). Statistical analysis was performed using 1-way ANOVA with Tukey's post-hoc test: ns for non-significant. The error bars represent the standard deviation measured for N=30 cells.

We used two different microscopy techniques (TEM and AFM) in order to analyze, on an individual particle scale, these morphological parameters.

3.1.1. Particle shape and size

For each strain, the dimensions of individual bacteria were measured by image analysis from TEM pictures and cells size in aqueous environments was confirmed by height measurement in AFM contact mode. As illustrated in Fig. 1, both Gram-negative strains (*E. coli* and *P. aeruginosa*) have the characteristic shape of a bacillus (rod), whereas the Gram-positive strain (*S. aureus*) has the shape of a coccus (sphere). The average smallest cell width for each strain in control conditions (physiological solution) is 0.91 ± 0.10 µm for *E. coli*, 0.79 ± 0.09 µm for *P. aeruginosa*, and 0.74 ± 0.11 µm for *S. aureus*. After antibiotic treatment as described in Section 2.2, no significant modification of cell size or morphology was observed by TEM image analysis (Fig. 1B). In our experimental conditions, the overall morphological characteristics of the cells and the absence of noticeable modification to size and shape after antibiotic treatment were confirmed by TEM and AFM observations.

3.1.2. Bacteria stiffness

Atomic Force Microscopy (AFM) was used to measure the nanomechanical properties of the bacterial cell wall. This measurement was realized in liquid media on living cells. With this technology, the nanomechanical properties of the cell wall of each strain were evaluated and the effect of antibiotic treatments was explored. From indentation measurements, the Young Modulus of the surface was deduced using the Hertz model. The Hertz model can be considered as a nanomechanical model reduced to its elementary ingredient i.e. one parameter describing macroscopically the stiffness of a cell. Using this model to treat the experimental data assumes that the characterized surface is homogeneous and massive. Knowing that bacteria are better described as pressurized non-homogeneous vessels, the Young Modulus values reached using this model are not actual ones but can be qualified as "apparent". Nevertheless, we considered in the present work that the relative variations of these apparent Young Modulus values can provide valuable interpretation of soft bacteria behavior during filtration. A decrease in the apparent Young Modulus means that for the same applied force, the tip indentation is smaller, characterizing softer bacteria. Moreover, the antibiotics we used in this study only target the cell wall peptidoglycan which is mainly responsible for the bacterial cell wall nanomechanical properties. Therefore, the apparent Young Modulus variations that we measured before and after antibiotic treatment can mainly be attributed to the cell wall stiffness modifications.

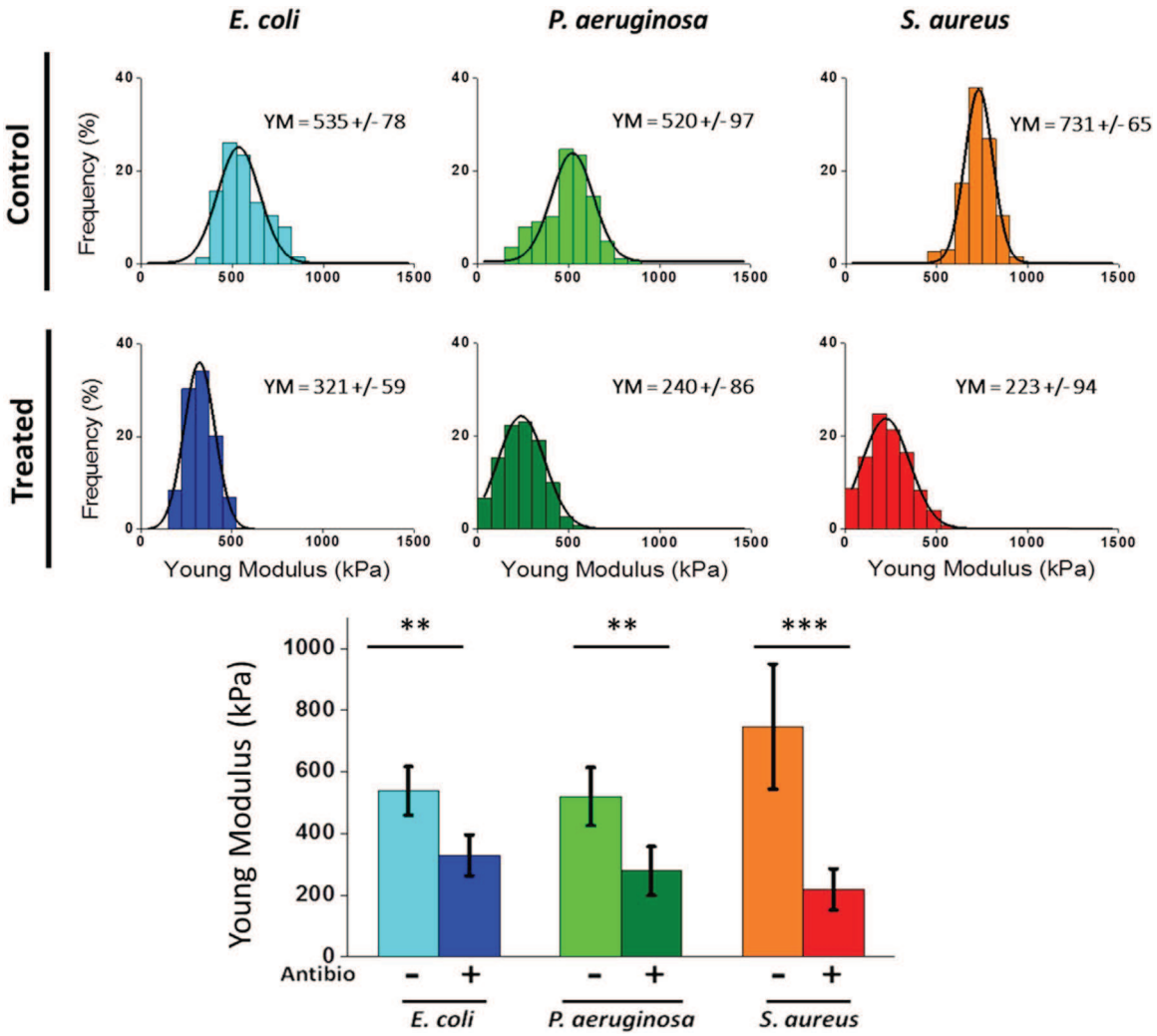

Fig. 2. AFM measurements of the cell surface stiffness in control conditions and after antibiotic treatment. Top: Illustration of representative distribution of apparent Young Modulus (YM) values (for N=1024 force curves) extracted from the elasticity map recorded with AFM force spectroscopy mode on the surface of one sampled bacteria cell. For each studied cell, YM median value was calculated by fitting a Gauss model (indicated by the black curves). Bottom: Comparative diagram of apparent Young Modulus mean values of the cell wall for the three bacterial strains and for the two challenged conditions (cell suspension in physiological solution named as control conditions noted – and after antibiotic treatment at MIC/2 for 90 min noted +). The error bars represent the standard deviation measured for N=9 cells resulting from three independent cultures. Statistical analysis was performed using 1-way ANOVA with Tukey's post-hoc test. ns for non-significant; ** for $P < 0.01$; *** for $P < 0.001$.

Results obtained in this study are reported in Fig. 2. In control conditions, force-spectroscopy revealed a difference in the bacteria stiffness between Gram-negative and Gram-positive strains. Gram-negative studied strains are more flexible, with apparent Young Modulus mean values of 539 ± 75 kPa for *E. coli* and 521 ± 56 kPa for *P. aeruginosa*. Gram-positive *S. aureus* is more rigid, with an apparent Young Modulus mean value of 748 ± 101 kPa. This higher value seems related to the thicker peptidoglycan layer that is present outside the cell membrane. For Gram-negative bacteria, the thickness of the peptidoglycan layer is around 2–6 nm [34], whereas Gram-positive bacteria present a thicker peptidoglycan layer around 15–30 nm [35].

After the antibiotic treatment, for all studied strains, AFM observations showed a significant decrease of the apparent Young Modulus value. This phenomenon was more significant for the Gram-positive bacteria (*S. aureus*) confirming that damage caused by the antibiotics on the cross-linkages between the peptidoglycan polymer chains were more important by comparison with Gram-negative bacteria cell wall alteration. In this latter case, the peptidoglycan layer is thinner and protected from the environment by the outer membrane. The apparent Young Modulus mean values after antibiotic treatment were found as 329 ± 67 kPa for *E. coli*, 279 ± 79 kPa for *P. aeruginosa* and 218 ± 67 kPa for *S. aureus*.

3.2. Bacterial transfer through the membrane

The bacterial concentration in the permeate (Cp), collected after each experimental run, was measured for every set of operating conditions (depending on bacterial strain, Cf, TMP and antibiotic treatment). In each case, the filtration experiment was run with a 0.4 µm pore size isopore membrane under sterile conditions. For the three studied strains, the results are shown in Fig. 3 in a histogram form, where Cp versus TMP was plotted for filtration of suspensions with increasing bacterial concentration.

3.2.1. Impact of operating conditions (bacteria strain, Cf and TMP)

As expected from previous works, we observed in this study that the three studied strains were able to pass through our model membrane, even if the membrane pore size was smaller than the smallest dimension of the bacteria cell. The magnitude of permeate contamination was specific to each strain and was dependent on the applied operating conditions.

Our results show that the *S. aureus* studied strain exhibits the highest retention rate by the membrane (or the lowest transfer rate) for

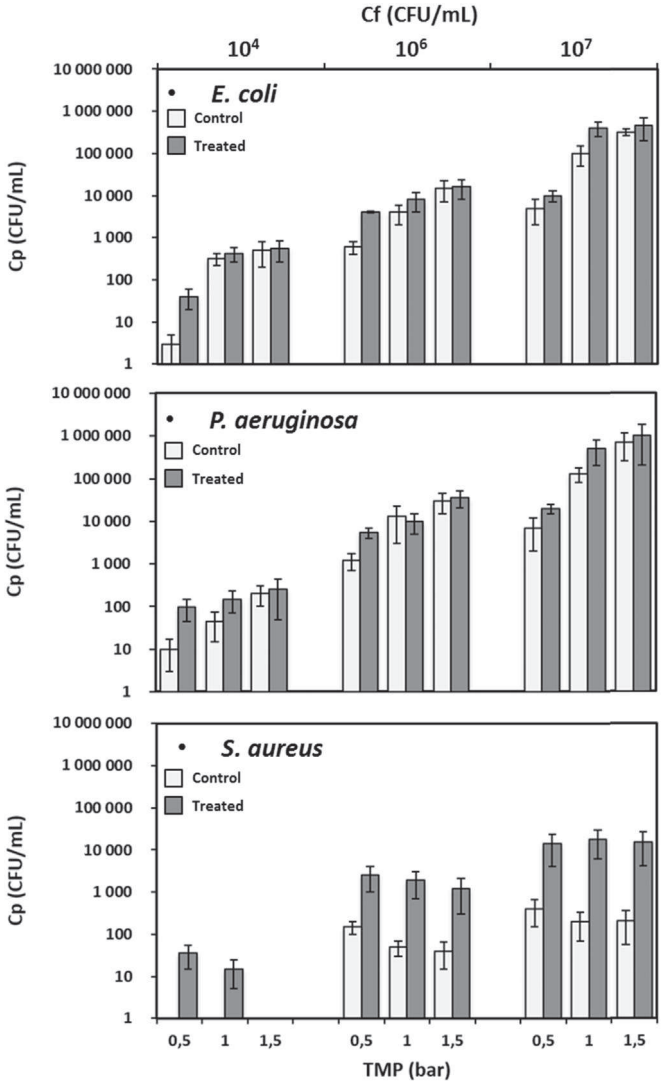

Fig. 3. Bacterial concentration in the permeate under various operating conditions during filtration runs with 0.4 µm membrane pore size. From top to bottom: evolution of the bacterial concentration in the permeate (Cp) as a function of the applied transmembrane pressure (TMP) during filtration of bacterial feed suspensions with increasing concentrations (Cf about 10^4, 10^6 and 10^7 CFU / mL) for *E. coli* CIP 54124, *P. aeruginosa* CIP 103467 and *S. aureus* CIP 53154 respectively. For each Cf and TMP, Cp was reported in both cases: control conditions and treated bacteria by contact with the antibiotic at the concentration of MIC/2.

every challenged condition, in comparison with the two Gram-negative strains. The specific behavior of *S. aureus* cannot be explained by the consideration of cell-size characteristics, since the smallest width of *S. aureus* and *P. aeruginosa* are equivalent (Section 3.1). To elucidate this phenomenon, the specific cell wall structure of the bacteria needs to be taken into account. As developed in the previous section, the nanomechanical properties of the three selected strains were studied by AFM. In control conditions, our results showed a correlation between the bacteria stiffness (expressed by the apparent Young Modulus value) and the Gram group. Gram-positive bacteria, such as *S. aureus*, are less deformable due to their thicker peptidoglycan layer. Therefore, in the same filtration conditions, this type of bacteria is better rejected by the membrane than Gram-negative bacteria which exhibit a thin and deformable layer of peptidoglycan.

To assess the influence of the bacterial feed concentration (Cf) on the cell transfer through the membrane structure, three increasing concentrations have been challenged: 10^4, 10^6 and 10^7 CFU/mL. The results presented in Fig. 3 demonstrate that for a low filtered volume (absence or negligible deposit formation), increasing the feed concentration causes a significant amplification of the number of cells collected in the permeate whatever the strain. This result is obviously related to the probability of meetings between a cell and a membrane pore, which increases with the concentration of the bacterial suspension. At the lowest concentration (Cf: 10^4 CFU/mL), both Gram-negative studied strains, *E. coli* and *P. aeruginosa*, were found in permeate samples after the filtration of 50 mL of suspension. In contrast, the Gram-positive *S. aureus*, was not detected from the filtered fluid in control conditions. This difference in retention between Gram-negative and Gram-positive strains for a low concentration in the feed corresponds to the observations and conclusions of previous work [7]. When the bacterial concentration of the *S. aureus* suspension was higher than, or equal to, 10^6 CFU/mL, significant contamination was observed in the permeate. However, the effluent contamination by *S. aureus* was always lower than that of Gram-negative strains.

In order to investigate the evolution of the membrane retention as a function of TMP, a short-pressure range that covers the industrial applications of the microfiltration process was selected. As shown in Fig. 3, for both Gram-negative strains, an increase in applied TMP from 0.5 to 1 bar, led to a substantial intensification in the bacterial transfer. In the case of the *S. aureus* studied strain, we observed that TMP variations did not have a comparable effect. In the studied range (from 0.5 to 1.5 bar), the transfer of the Gram-positive strain slightly decreased with an increase in TMP, excepted for the highest concentration (10^7 CFU/mL) after bacteria treatment by the antibiotic. For the highest concentration studied, cellular aggregates could be formed in the *S. aureus* suspension especially in stress conditions such as the ones encountered during filtration operation. This phenomenon must be amplified for *S. aureus* suspension exposed to subinhibitory concentrations of antibiotics [36]. Higher LRV for the highest concentration studied with *S. aureus* could be then a consequence of this specific behavior. This phenomenon has been confirmed by Scanning Electron Microscopy observation of the membrane surface after *S. aureus* filtration (data not shown). This result, which contrasts to the Gram-negative behavior, will be discussed in Section 3.2.3.

3.2.2. Impact of bacteria cell wall alteration (antibiotic treatment)

In Section 3.1.2, we measured the impact of antibiotic treatment on the nanomechanical properties of the bacteria cell wall by experiments conducted by AFM, a treatment which induced a reduction of the stiffness of the cell wall. For this study, the antibiotic treatment was conducted over a short time period (90 min) and at a low concentration (MIC/2), in order to avoid bacteria mortality during the filtration experiments. For the three bacterial strains, bacteria transfer through membrane pores was amplified after antibiotic treatment in comparison with the control conditions as shown in Fig. 3. This difference in retention efficiency was always more significant at the lowest challenged TMP (0.5 bar). When TMP was increased, the effect on the transfer of the antibiotic treatment was less significant for the two Gram-negative strains: despite the fact that *E. coli* and *P. aeruginosa* were respectively exposed to amoxicillin and ticarcillin, no significant amplification of the bacteria concentration in the permeate was observed at the highest challenged TMP of 1.5 bar. For *S. aureus*, a suspension treated with amoxicillin, we observed a different behavior: the transfer magnitude of the treated bacteria was significantly increased in comparison to the control conditions. At the lowest feed concentration (10^4 CFU/mL), when a total retention was observed for the *S. aureus* suspension under control conditions, the antibiotic treatment induced a high passage of *S. aureus* cells through the 0.4 µm membrane pores. At higher feed concentrations, this specific behavior was still observed: *S. aureus* cells treated with amoxicillin exhibited an amplified transfer. Finally, the transfer after antibiotic treatment did not increase with TMP, similarly to the control conditions, in the range of 0.5–1.5 bar.

To sum up, our results showed that the three studied bacterial

strains have the ability to penetrate through a 0.4 μm membrane pore size and that the magnitude of the effluent contamination is correlated to the transmembrane pressure and the feed concentration. Also, this work demonstrated that the antibiotic treatment of Gram-negative studied bacteria induces the highest diminution of the retention efficiency of the membrane for the lowest challenged transmembrane pressure (0.5 bar) and, that the impact of the chemical exposure is reduced when the transmembrane pressure is increased. Concerning Gram-positive bacteria filterability, the studied *S. aureus* strain exhibited a different and negligible sensitivity to the applied pressure in the challenged range. Moreover, the difference between the retention efficiency for the three bacteria strains was demonstrated to be linked to morphological and mechanical properties of individual bacteria cells. In this context, the next section is dedicated to connecting the measured structural characteristics of the cells (dimension and stiffness) and the observed selectivity of the filtration experiments.

3.2.3. Cell transfer model

We have collected data on filtration retention efficiency for three bacterial strains and a range of feed concentrations or applied transmembrane pressures. Furthermore, we have explored the impact of antibiotic treatment on the filter cell removal efficiency. To correlate the data collected on a microscopic scale, such as morphological properties of the bacteria, and the retention measured on a macroscopic scale during dead-end filtration experiments, we have developed a simplified theoretical approach. The main objective was to related the transfer magnitude to the cell properties and to the filtration conditions. The transfer model is assuming that the membrane selectivity towards bacteria is mainly controlled by a deformation mechanism involving a stretching of the cell. The approach compares the driving force provided by the filtration process (due to the pressure gradient across the membrane) and the force needed to stretch the bacteria cell envelope to define if the bacteria can enter inside the pore.

When a bacteria cell is immobilized at the entrance of a pore, the object is subjected to the TMP applied to the filtration process. In our experimental conditions, the bacteria cell that is present at the entrance of one cylindrical pore of diameter 0.4 μm can undergo a substantial deformation, allowing the bacteria to penetrate inside the pore and then, migrate through the filter. This process of deformation is briefly summarized in Fig. 4.

At the initial state in suspension, the bacteria cell is described by the surface/volume ratio (noted S_0/V_0) calculated with the length L_0 and the radius R_0 of the cell. When the bacteria penetrate inside the membrane pore, the cell has to adopt a new shape which is dependent on the cylindrical geometry of the pore. The new dimensions of the deformed bacterial cell, inside a pore with a radius R_p, were defined by the ratio S_d/V_d calculated with the length L_d and the radius R_d of the cell inside the pore.

For the development of the bacteria transfer model, the following assumptions were made:

(1) Before the deformation step, the rod-shaped bacteria were represented by a spherocylinder (two hemispheres and one cylinder) and the coccus bacteria by a sphere,
(2) The cell present inside the pore was represented by a spherocylinder and the bacteria length has to be smaller than the pore depth ($L_d < L_m$ where L_m is the membrane thickness known from the manufacturer as 20 μm),
(3) Deformed bacteria cell inside the membrane pore fills the entire space available ($R_d=R_p$),
(4) Deformation of the bacterial cell is carried out by a stretching mechanism: the volume of the cell was assumed constant ($V_0=V_d$), whereas the cell surface increases during the deformation,
(5) The bacterial cell surface was defined as an elastic material which has a limit to the stretching, in the order of 300% before breaking [37]. As a consequence, the S_d/S_0 ratio cannot exceed the value of 3.

In the literature, different assumptions are used to model the cell deformation through a pore or a microcapillary [4,20–24]. It is frequently supposed that cell membrane surface is constant during the transfer by deformation simultaneously with a constant cell volume because the intracellular fluid is assumed as incompressible [21–24]. Recent studies explored the possibility of cell volume alteration during the deformation due to the pressure difference on both sides of bacterial cell wall [4,20]. In the present study, we proposed a model assuming a constant cell volume and an increase of the surface of the bacteria during the deformation process.

In the case of a rod shape bacteria, the S_0 and V_0 terms correspond to the initial surface and volume of the cell in suspension, and they are defined as follows:

$$S_0=4\pi R_0^2+2\pi R_0 L_0 \tag{1}$$

$$V_0=\frac{4}{3}\pi R_0^3+\pi R_0^2 L_0 \tag{2}$$

When the bacteria penetrate a pore with a radius R_p, based on assumption (2), the surface and the volume of the deformed cell S_d and V_d become:

$$S_d=4\pi R_p^2+2\pi R_p L_d \tag{3}$$

$$V_d=\frac{4}{3}\pi R_p^3+\pi R_p^2 L_d \tag{4}$$

According to assumption (4), the cell volume is constant during the deformation steps, leading to the following relationship used to calculate the length L_d of the deformed cell inside the membrane pore

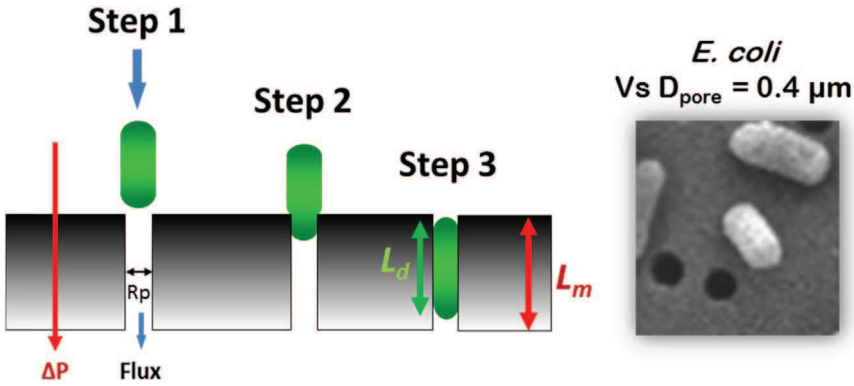

Fig. 4. Schematic view of the transfer by deformation of one bacteria cell through a pore under the action of filtration flux imposed by the transmembrane pressure. Step 1: initial state of the bacteria cell in the feed suspension. Step 2: cell deformation by stretching at the pore entrance. Step 3: deformed cell inside the pore of the membrane. Image (right): illustration of Step 2 observed by Scanning electron microscopy with *E. coli* (CIP 54124) on 0.4 μm membrane.

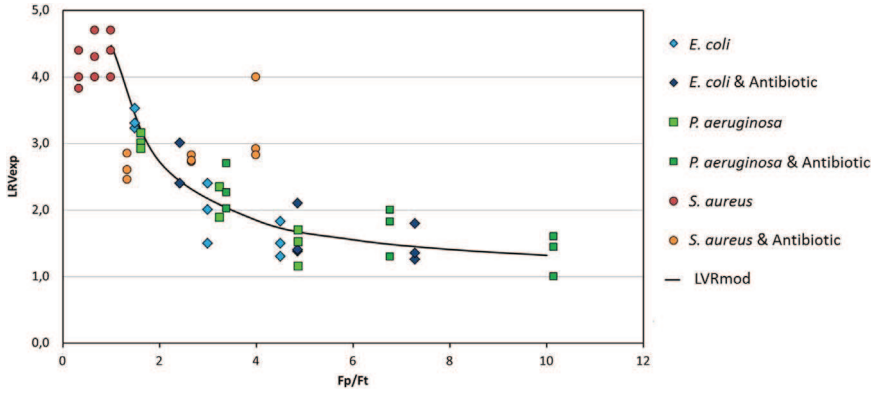

Fig. 5. Evolution of the experimental LRV as a function of the force ratio (denoted as Fp/Ft) between the force applied by the transmembrane pressure Fp and the tension force Ft required to achieve the deformation of the bacteria cell, that is just sufficient for the cell to penetrate the pore. (For interpretation of the references to color in this figure, the reader is referred to the web version of this article).

as a function of the pore size R_p:

$$L_d = \frac{\frac{4}{3}(R_0^3 - R_p^3) + R_0^2 L_0}{R_p^2} \tag{5}$$

Using Eqs. (3) and (5), one can obtain an expression of the deformed cell surface S_d based on parameters, such as the initial cell dimensions and the membrane pore size:

$$S_d = \frac{1}{R_p}\left(\frac{4}{3}\pi R_p^3 + \frac{8}{3}\pi R_0^3 + 2\pi R_0^2 L_0\right) \tag{6}$$

Hypotheses 2 and 5 have been controlled with numerical values: for all the calculation performed, the values of L_d were less than 9 μm and the calculated ratio S_d/S_0 was less than 2.

Based on assumption 4, it is possible to express the surface tension of the bacteria inside the membrane pore as a function of the deformation undergone by the cell. Cell surface tension, denoted as T in this study, can be written as:

$$T = e\ E\ \mathrm{D} \tag{7}$$

where e is the peptidoglycan layer thickness of the bacteria cell wall, E is the apparent Young Modulus value and D is the cell deformation factor. This last factor normalizes the difference between the cell surface at the initial state and the cell surface inside the pore, according to the following equation:

$$D = \frac{S_d - S_0}{S_0} \tag{8}$$

Thus, the cell surface tension, T, is a function of the membrane pore size, and of the morphological and nanomechanical properties of the bacteria cell; parameters which have been experimentally determined in the first part of this work, or extracted from the literature. Numerical values of the thickness of the peptidoglycan layer of each bacteria species were found as 6.4 nm for *E. coli* [34], 2.4 nm for *P. aeruginosa* [34] and 30 nm for *S. aureus* [35].

The force required to achieve the deformation just sufficient for the penetration of the cell in the pore of radius R_p, denoted Ft, is related to the cell wall tension T as follow:

$$Ft = 2\pi R_p T \tag{9}$$

This force can be compared to the mechanical force applied on the cell section at the entrance of this pore due to the transmembrane pressure:

$$Fp = \pi R_p^2 TMP \tag{10}$$

The force ratio Fp/Ft (the ratio between the force delivered by the filtration process and the force required for the cell deformation), is then a key condition for the cell transfer through the membrane. For Gram-negative strains (*E. coli* and *P. aeruginosa*) in all challenged conditions, the values of the Fp/Ft ratio are higher than 1 due to the low values of the tension force, Ft, because of the small thickness of the peptidoglycan layer and the high stiffness of this type of cell (explained by the small YM median values). For Gram-negative strains, antibiotic treatments induce additional Ft diminution. For the studied Gram-positive strain *S. aureus*, the value of the Fp/Ft ratio is, in control conditions, less than 1 when the antibiotic treatment with amoxicillin induces an increase in the Fp/Ft ratio, which becomes greater than 1.

Experimentally, the filtration efficiency has been measured for each bacteria strain and for a large range of parameters (TMP, Cf and antibiotic treatment). The membrane retention efficiency was calculated using the log reduction value (LRV) according to the following relationship:

$$LRV = \log\left(\frac{Cf}{Cp}\right) \tag{11}$$

where Cf and Cp respectively are the bacterial feed and permeate concentration (CFU/mL).

The experimental LRV (LRVexp) as a function of the force ratio Fp/Ft is plotted in Fig. 5. We can observe a correlation between the filtration efficiency and the calculated force balance (given in Supplementary information). For the Gram-negative strains (*E. coli* and *P. aeruginosa*), which expose in all challenged conditions values of Fp/Ft ratio greater than 1, we can notice that the selectivity expressed in LRV exhibits a very strong relationship with the Pressure/Tension force ratio: the higher the driving force Fp compared to the tension Ft, the lower the separation efficiency (the transmission of bacteria is increased). Alternatively, the LRVexp measured with the Gram-positive *S. aureus* strain (orange and red dots) does not seem to follow the same trend. For this strain in control conditions (red dots), the force ratio Fp/Ft is less than 1 for all challenged conditions (various Cf and TMP). Therefore, the LRV is nearly constant, which can be explained by the fact that the driving force remains lower than the tension force required for cell deformation. In the specific case where the LRV is linear for a Fp/Ft ratio between 0 and 1, we can assume that the bacteria deformation does not occur and the transfer is then controlled by the bacteria/pore sizes ratio. For the *S. aureus* strain treated with antibiotics, the Fp/Ft ratio becomes higher than 1 (yellow dots) as for Gram-negative strains, but the experimental points are much more dispersed and away from the numerical trend curve. This particular behavior seems to follow a different trend with a slight increase of the LRVexp with the Fp/Ft ratio. This is consistent with the increase in retention efficiency with the applied pressure shown in Fig. 3. This phenomenon remains to be elucidated and only one hypothesis is presented here. Excepted for the differences in cell envelope structure, one other specific property of Gram-positive strains is the potent

internal pressure of the cell according to the external constraint imposed. Indeed, Gram-positive cells such as *S. aureus* exhibit a high turgor pressure (Pcell in the range 4–6 bar) [38] which could limit the phenomena of cell stretching at the entrance of the pore. In contrast, *E. coli* cells have a much lower turgor pressure (Pcell around 0.1 bar) which is not a limiting parameter for cell deformation. Thus, in the case where the turgor pressure of the cell is high and greater than the applied transmembrane pressure (Pcell > TMP), the internal pressure could counter the cell deformation, and the transfer through the membrane pore could be blocked. Retention may even be amplified with the increasing TMP, the cell forming a plug at the entrance of the pore. Plugging is dependent on TMP due to the mechanism of compression of the cell which collapses at the entrance of the pore. Higher is TMP, higher is the cell compression. We assumed that this increase in cell compression at the entrance of the pore leads to the total blockage of this last. One blocked pore does not allow anymore transfer of bacteria cell through the membrane resulting in an increase of the apparent membrane selectivity.

In the case of Gram-negative strains, we have gone further into the analysis of the results by considering the effect of the force ratio Fp/Ft on the cell transfer probability. First, we have considered a Boltzmann distribution, for assessing the probability of bacteria transfer as a function of the Fp/Ft ratio such as:

$$P = \alpha e^{-\frac{\beta}{Fp/Ft}} = \alpha e^{-\beta\frac{Ft}{Fp}} \quad (12)$$

where α and β are adjustable constant parameters. Thus, for a value of the Fp/Ft ratio which tends to an infinite value (or if Ft/Fp tends to zero), corresponding to the cases where TMP is much higher than the tension T, the passage probability P reaches a maximum and is equal to alpha. In opposition, for a Fp/Ft ratio which tends to 0, in the case where the tension force is well higher than the TMP forces, the transfer probability is reaching a minimal value close to zero.

In our work, we assumed that the limiting step of this selectivity mechanism is the penetration of the bacteria into the membrane pore. Once inside the pore, the cell transfer to the permeate phase was considered as complete and the effluent contamination effective. This hypothesis is consistent with the results obtained by Secomb and Hsu [24]. These authors proposed a numerical simulation of red blood cells transfer through micrometric pores and showed that the time required for the introduction of the cell represents 50–75% of the total time required for the transfer.

In this assumption, the probability P can be used to numerically deduce the log reduction value (noted as LRVmod for model LRV) calculated only from challenged bacterial strain characteristics and applied operating conditions (bacteria cell morphological properties, membrane pore size, TMP and Cf), defined by the following relationship:

$$LRV\ \mathrm{mod} = -\log(P) \quad (13)$$

Fig. 6 compares experimental and calculated LRV for both Gram-negative strains (*E. coli* and *P. aeruginosa*) for all the challenged

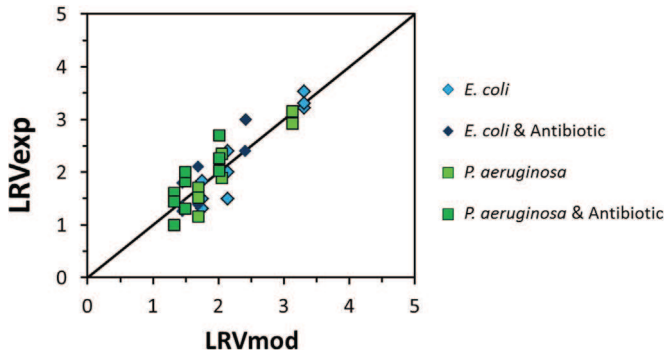

Fig. 6. Evolution of the experimental LRV versus the calculated LRV.

conditions. The parameters α and β have been fixed by the least squares method, respectively as 0.106 and 8.062. The LRVmod values (given in Supplementary information) are shown in Fig. 5 so that a numerical trend curve can be plotted on the graph. In the case of Gram-negative strains, our model shows that the cell transfer through the membrane pore by deformation can be correlated to force ratio between the cell surface tension and the transmembrane pressure, where the mechanical energy applied can lead to the cell deformation which allows the Gram-negative strains to pass through the pore.

The hypothesis and model presented in the current study allow to describe the transfer of a population of Gram-negative cells by deformation through the membrane pore with a simple approach. Taking into account information such as the transmembrane pressure and surface tension of the bacterial cell, in defined environmental conditions, it is possible to anticipate the magnitude of the permeate contamination.

If we come back to the choice of the Hertz model to treat AFM data, point discussed in Section 3.1.2, the rather good agreement observed between calculated and experimental LRV allows to conclude that the apparent Young modulus is a relevant parameter to depict the effect of cell deformability on the transfer through a membrane pore.

The specific behavior of Gram-positive strains that is not described by our model confirms the existence of a different selectivity mechanism for this type of cell. Further experiments should be considered in order to observe the effects of transmembrane pressure on the filterability of this type of bacteria.

4. Conclusion

The operative parameters, such as the transmembrane pressure or the bacterial concentration in the feed are two factors that impact the magnitude of the transfer of bacteria. Nevertheless, the structural characteristics of the cell, coupled to the stiffness of the cell wall explain the specific selectivity mechanism adapted to each living cell. Indeed, when antibiotics were present in suspension medium, affecting the mechanical properties of bacterial cell wall by decreasing the rigidity, we observed an amplification of the contamination in the permeate phase. In this study, we considered that the deformation of the bacteria cell during the transfer is mainly due to a stretching mechanism of the cell wall without any volume change or cytoplasm leakage. Our results demonstrate a strong correlation between the experimental membrane efficiency (expressed in LRV) and the value of the surface tension, calculated using a simplified numerical model for the three studied strains. The surface tension, as we have described, is expressed as a function of all the morphological characteristics of the bacteria cell: the thickness of the peptidoglycan layer and the stiffness of the cell wall, the cell deformation factor (which includes the smallest cell size and the membrane pore size). The developed model allowed to connect the parameters influencing the bacteria retention. It links the membrane selectivity (on a macroscale) of the Gram-negative suspensions to the microscopic information about individual particles. Concerning the Gram-positive *S. aureus* strain, this model is limited in its description of the experimental observations: the retention mechanism of this cell type may be limited by the high turgor pressure, in the assay conditions.

Acknowledgments

This work benefitted from the assistance of the Multiscale Electron Imaging platform (METi) of the FRBT of the University of Toulouse. The authors are also grateful for the financial support from Region Midi-Pyrénées (grant n°12052817) and for the technical support from Maëlle Monier and Alexandre Bacou.

Appendix A. Supplementary material

Supplementary data associated with this article can be found in the online version at http://dx.doi.org/10.1016/j.memsci.2016.10.023.

References

[1] M.W. Jornitz, Sterile Filtration, Springer-Verlag, Berlin/Heidelberg, 2006. http://dx.doi.org/10.1007/b101405.

[2] T.W. Secomb, R. Hsu, A.R. Pries, Motion of red blood cells in a capillary with an endothelial surface layer: effect of flow velocity, Am. J. Physiol. Heart Circ. Physiol. J. Physiol. Heart Circ. Physiol. 5051 (2001) 629–636.

[3] Y. Wang, F. Hammes, M. Düggelin, T. Egli, Influence of size, shape, and flexibility on bacterial passage through micropore membrane filters, Environ. Sci. Technol. 42 (2008) 6749–6754. http://dx.doi.org/10.1021/es800720n.

[4] T. Suchecka, W. Piątkiewicz, T.R. Sosnowski, Is the cell retention by MF membrane absolutely safe – a hypothetical model for cell deformation in a membrane pore, J. Membr. Sci. 250 (2005) 135–140. http://dx.doi.org/10.1016/j.memsci.2004.08.035.

[5] M.T. Cabeen, G. Charbon, W. Vollmer, P. Born, N. Ausmees, D.B. Weibel, C. Jacobs-Wagner, Bacterial cell curvature through mechanical control of cell growth, EMBO J. 28 (2009) 1208–1219. http://dx.doi.org/10.1038/emboj.2009.61.

[6] S.B. Sadr Ghayeni, P.J. Beatson, A.J. Fane, R.P. Schneider, Bacterial passage through microfiltration membranes in wastewater applications, J. Membr. Sci. 153 (1999) 71–82. http://dx.doi.org/10.1016/S0376-7388(98)00251-8.

[7] N. Lebleu, C. Roques, P. Aimar, C. Causserand, Role of the cell-wall structure in the retention of bacteria by microfiltration membranes, J. Membr. Sci. 326 (2009) 178–185. http://dx.doi.org/10.1016/j.memsci.2008.09.049.

[8] A. Helling, A. Kubicka, I.A.T. Schaap, M. Polakovic, B. Hansmann, H. Thiess, J. Strube, V. Thom, Passage of soft pathogens through microfiltration membranes scales with transmembrane pressure, J. Membr. Sci. (2016). http://dx.doi.org/10.1016/j.memsci.2016.08.016.

[9] J.G. Stockner, M.E. Klut, W.P. Cochlan, Leaky filters: a warning to aquatic ecologists, Can. J. Fish. Aquat. Sci. 47 (1990) 16–23. http://dx.doi.org/10.1139/f90-002.

[10] C.F. Nnadozie, J. Lin, R. Govinden, Selective isolation of bacteria for metagenomic analysis: impact of membrane characteristics on bacterial filterability, Biotechnol. Prog. 31 (2015) 853–866. http://dx.doi.org/10.1002/btpr.2109.

[11] T.J. Silhavy, D. Kahne, S. Walker, The bacterial cell envelope, Cold Spring Harb. Perspect. Biol. 2 (2010) a000414. http://dx.doi.org/10.1101/cshperspect.a000414.

[12] W.W. Baldwin, M.J. Sheu, P.W. Bankston, C.L. Woldringh, Changes in buoyant density and cell size of Escherichia coli in response to osmotic shocks, J. Bacteriol. 170 (1988) 452–455.

[13] F. Gaboriaud, S. Bailet, E. Dague, F. Jorand, Surface structure and nanomechanical properties of Shewanella putrefaciens bacteria at two pH values (4 and 10), J. Bacteriol. 187 (2005) 3864–3868. http://dx.doi.org/10.1128/JB.187.11.3864.

[14] A.-C. Chien, N.S. Hill, P.A. Levin, Cell size control in bacteria, Curr. Biol. 22 (2012) R340–R349. http://dx.doi.org/10.1016/j.cub.2012.02.032.

[15] C. Formosa, M. Grare, R.E. Duval, E. Dague, Nanoscale effects of antibiotics on P. aeruginosa, Nanomed. Nanotechnol. Biol. Med. 8 (2012) 12–16. http://dx.doi.org/10.1016/j.nano.2011.09.009.

[16] C. Formosa, M. Grare, E. Jauvert, A. Coutable, J.B. Regnouf-de-Vains, M. Mourer, R.E. Duval, E. Dague, Nanoscale analysis of the effects of antibiotics and CX1 on a Pseudomonas aeruginosa multidrug-resistant strain, Sci. Rep. 2 (2012) 575. http://dx.doi.org/10.1038/srep00575.

[17] G. Francius, O. Domenech, M.P. Mingeot-Leclercq, Y.F. Dufrêne, Direct observation of Staphylococcus aureus cell wall digestion by lysostaphin, J. Bacteriol. 190 (2008) 7904–7909. http://dx.doi.org/10.1128/JB.01116-08.

[18] K. Cronholm, S. Bates, N. Nguyen, A. Leahy, M. Blanchard, K.R. Lentine, Validation of a microbiological method using Acholeplasma laidlawii for assessing performance of microporous membranes for mycoplasma clearance, PDA J. Pharm. Sci. Technol. 63 (2009) 438–461 http://www.ncbi.nlm.nih.gov/pubmed/20158050.

[19] M. Folmsbee, G. Howard, M. McAlister, Nutritional effects of culture media on mycoplasma cell size and removal by filtration, Biologicals 38 (2010) 214–217. http://dx.doi.org/10.1016/j.biologicals.2009.11.001.

[20] M. Szwast, T. Suchecka, W. Piatkiewicz, Mathematical model for biological cell deformation in a cylindrical pore, Chem. Process Eng. – Inz. Chem. I Process 33 (2012) 385–396. http://dx.doi.org/10.2478/v10176-012-0034-x.

[21] D.J. Quinn, I. Pivkin, S.Y. Wong, K.H. Chiam, M. Dao, G.E. Karniadakis, S. Suresh, Combined simulation and experimental study of large deformation of red blood cells in microfluidic systems, Ann. Biomed. Eng. 39 (2011) 1041–1050. http://dx.doi.org/10.1007/s10439-010-0232-y.

[22] P.J. Abatti, Determination of the red blood cell ability to traverse cylindrical pores, IEEE Trans. Biomed. Eng. 44 (1997) 209–212. http://dx.doi.org/10.1109/10.554767.

[23] P. Preira, M.-P. Valignat, J. Bico, O. Théodoly, Single cell rheometry with a microfluidic constriction: quantitative control of friction and fluid leaks between cell and channel walls, Biomicrofluidics 7 (2013) 024111. http://dx.doi.org/10.1063/1.4802272.

[24] T.W. Secomb, R. Hsu, Analysis of red blood cell motion through cylindrical micropores: effects of cell properties, Biophys. J. 71 (1996) 1095–1101. http://dx.doi.org/10.1016/S0006-3495(96)79311-6.

[25] F. Pillet, L. Chopinet, C. Formosa, E. Dague, Atomic Force Microscopy and pharmacology: from microbiology to cancerology, Biochim. Biophys. Acta – Gen. Subj. 1840 (2014) 1028–1050. http://dx.doi.org/10.1016/j.bbagen.2013.11.019.

[26] V. Dupres, D. Alsteens, G. Andre, Y.F. Dufrêne, Microbial nanoscopy: a closer look at microbial cell surfaces, Trends Microbiol 18 (2010) 397–405. http://dx.doi.org/10.1016/j.tim.2010.06.004.

[27] K.J. Kim, P.V.V. Stevens, Hydraulic and surface characteristics of membranes with parallel cylindrical pores, J. Membr. Sci. 123 (1997) 303–314. http://dx.doi.org/10.1016/S0376-7388(96)00232-3.

[28] I. Wiegand, K. Hilpert, R.E.W. Hancock, Agar and broth dilution methods to determine the minimal inhibitory concentration (MIC) of antimicrobial substances, Nat. Protoc. 3 (2008) 163–175. http://dx.doi.org/10.1038/nprot.2007.521.

[29] Standard Test Method for Determining Bacterial Retention of Membrane Filters Utilized for Liquid Filtration. ASTM Standard F838-05, Philadelphia, PA, 2013.

[30] G. Francius, B. Tesson, E. Dague, V. Martin-Jézéquel, Y.F. Dufrêne, Nanostructure and nanomechanics of live Phaeodactylum tricornutum morphotypes, Environ. Microbiol. 10 (2008) 1344–1356. http://dx.doi.org/10.1111/j.1462-2920.2007.01551.x.

[31] E. Dague, E. Jauvert, L. Laplatine, B. Viallet, C. Thibault, L. Ressier, Assembly of live micro-organisms on microstructured PDMS stamps by convective/capillary deposition for AFM bio-experiments, Nanotechnology 22 (2011) 395102. http://dx.doi.org/10.1088/0957-4484/22/39/395102.

[32] C. Formosa, F. Pillet, M. Schiavone, R.E. Duval, L. Ressier, E. Dague, Generation of living cell arrays for atomic force microscopy studies, Nat. Protoc. 10 (2015) 199–204. http://dx.doi.org/10.1038/nprot.2015.004.

[33] H.Hertz, Ueber die Berührung fester elastischer Körper., J. Für Die Reine Und Angew. Math., 92 (n.d.), pp. 156–171.

[34] V.R.F. Matias, A. Al-Amoudi, J. Dubochet, T.J. Beveridge, Cryo-transmission electron microscopy of frozen-hydrated sections of escherichia coli and pseudomonas aeruginosa, J. Bacteriol. 185 (2003) 6112–6118. http://dx.doi.org/10.1128/JB.185.20.6112-6118.2003.

[35] W. Vollmer, D. Blanot, M.A. De Pedro, Peptidoglycan structure and architecture, FEMS Microbiol. Rev. 32 (2008) 149–167. http://dx.doi.org/10.1111/j.1574-6976.2007.00094.x.

[36] J. Haaber, M.T. Cohn, D. Frees, T.J. Andersen, H. Ingmer, Planktonic aggregates of Staphylococcus aureus protect against common antibiotics, PLoS One 7 (2012) 1–12. http://dx.doi.org/10.1371/journal.pone.0041075.

[37] A.L. Koch, S. Woeste, Elasticity of the sacculus of Escherichia coli, J. Bacteriol. 174 (1992) 4811–4819.

[38] X. Yao, J. Walter, S. Burke, S. Stewart, M.H. Jericho, D. Pink, R. Hunter, T.J. Beveridge, Atomic force microscopy and theoretical considerations of surface properties and turgor pressures of bacteria, Colloids Surf. B Biointerfaces 23 (2002) 213–230. http://dx.doi.org/10.1016/S0927-7765(01)00249-1.